NOTES AND CORRESPONDENCE

Sampling Requirements for the Surface Wind Field over the Tropical Pacific Ocean*

L. J. MANGUM, S. P. HAYES, AND L. D. STRATTON

Pacific Marine Environmental Laboratory, National Oceanic and Atmospheric Administration, Seattle, Washington

7 October 1991 and 26 March 1992

ABSTRACT

Moored wind measurements at near-equatorial locations along 110°W, 125°W, 140°W, 170°W, and 165°E are used to investigate the space-time variability of the tropical Pacific wind field. These measurements complement previous studies that relied on island winds in the central Pacific or a few moored measurements in the eastern Pacific. Results indicate that the energetic portion of the zonal and meridional wind is significantly coherent over meridional scales of about 200 km and zonal scales of 1500 km. Even at these separations the estimated coherence often accounts for less than 50% of the variance. Temporal subsampling indicated (in agreement with previous studies) that at least ten samples per month were required to resolve monthly wind speed to within 1 m s^{-1} in the eastern equatorial Pacific. West of the date line and in the intertropical convergence zone (ITCZ), nearly daily sampling was required. Investigation showed that little error in the daily average of derived quantities such as wind speed and stress was associated with computing these variables from daily vector averages of the wind components rather than from hourly values of the components that were subsequently averaged.

1. Introduction

Describing, understanding, and modeling the low-frequency evolution of the tropical Pacific Ocean require accurate information on the surface wind forcing. Harrison et al. (1989, 1990) demonstrated that five different surface wind products, each of which purported to represent the monthly mean wind field over the tropical Pacific, yielded significantly different general circulation model (GCM) simulations of the 1982–83 El Niño–Southern Oscillation (ENSO) event. In sea surface temperature (SST), these differences were often as large as the ENSO anomalies. Similar results held for simulations of the 1986–87 ENSO event (Harrison 1990, personal communication) and of the annual cycle (Harrison 1992). These GCM studies demonstrate that accurate representation of the surface wind forcing is crucial in order to model the tropical ocean's response.

Much of the historical information on the surface wind field in the tropics comes from ship reports. These reports vary in quality and in temporal and spatial distribution. Halpern (1988a) noted that if the 106-yr global wind dataset used by Hellerman and Rosenstein (1983) was uniformly distributed in time, then each 2° × 2° area centered on the equator in the Pacific Ocean would only have about 0.5 observations per month. Similarly, Reynolds et al. (1989) found that even in the modern datasets most of the tropical Pacific had less than five ship observations each month. Halpern (1988a) used continuous, year-long in situ surface wind measurements from moored buoys along the equator at 95°, 110°, and 152°W to demonstrate that at least ten samples per month are required in order to obtain monthly mean wind speeds to an accuracy of 1.0 m s^{-1}. Resolution of the weekly to monthly wind variability, which can lead to large thermocline and surface dynamic height perturbations (e.g., Lukas et al. 1985; McPhaden et al. 1988), requires even more dense temporal sampling. Legler (1991) found that five to eight samples in a 5-day period were required to obtain 1.0 m s^{-1} accuracy in equatorial wind components at 95° and 152°W.

High-temporal-resolution wind fields are available from tropical Pacific islands, principally those centered near the date line (Harrison and Luther 1990). These data also provide estimates of zonal and meridional coherence scales. Near the equator, the most energetic zonal-wind variability is in a broad band with periods of about 3–60 days; the meridional-wind variance is about one-half of the zonal variance and is centered in the 3–6-day period band. Coherence calculations show significant zonal-wind coherence over about 200–300 km meridionally and 1000–1500 km zonally. The meridional-wind components tend to be less coherent.

* Contribution No. 1284 from NOAA's Pacific Marine Environmental Laboratory.

Corresponding author address: Dr. Stanley P. Hayes, NOAA, Pacific Marine Environmental Laboratory, NOAA Bldg. No. 3, Seattle, WA 98115.

These scales appear reasonable for the central equatorial Pacific Ocean from about 160°W to 170°E where most of the islands occur. At other longitudes, the wind regime may be significantly different. In the region from 95° to 140°W, Halpern (1988b) found no significant coherence between buoy winds measured on the equator with zonal separations of 1650 km and greater.

In this paper, we use in situ wind measurements from moored buoys to examine the temporal and spatial structure of the wind field at locations in the eastern (110° and 125°W), central (140° and 170°W), and western (165°E) Pacific. Measurement sites were along the equator and, at some longitudes, extended to 5°S and 9°N. At least 1 year of data was used at each location. The emphasis of the study is to use these new wind data to assist in establishing the design criteria for a surface wind measurement array in the tropical Pacific. These results extend the previous analyses of Halpern (1988a, 1988b) and Harrison and Luther (1990).

2. Wind time series and spectra

Time series of the wind measurements analyzed here are shown in Figs. 1–4. The equatorial time series in Fig. 1 is repeated in Figs. 2–4 in conjunction with the off-equatorial measurements along 110°W, 140°W, and 165°E. Measurements at the equatorial sites 110°W, 140°W, and 165°E were made using a vector-averaging wind recorder (VAWR) mounted on a surface-following toroid float at the top of current-measuring moorings. The VAWR system is described in Halpern (1988a). Briefly, wind direction is measured by a 9-cm × 17-cm balanced wind vane, and wind speed is measured by a three-cup anemometer. Speed and direction are measured nearly continuously and vector averaged at 15-min intervals. The 15-min-average data are internally recorded. Measurements are at a height of 3.8 m above the sea surface. In Figs. 1–4, the 15-min data have been vector averaged to daily values for display.

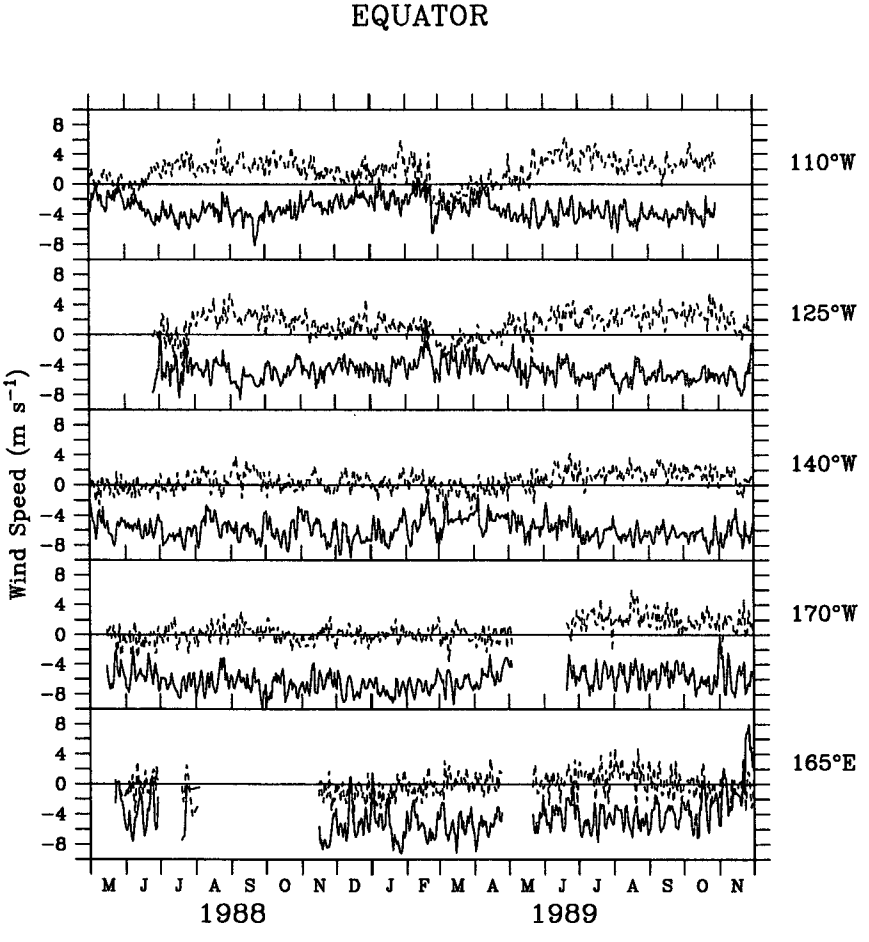

FIG. 1. Time series of daily averaged wind components (solid line is zonal wind, u is positive toward the east; broken line is meridional wind, v is positive toward the north) for measurements along the equator used in this study. Longitudes given are the nominal locations of the moorings. Actual deployment locations varied by up to 60 nm.

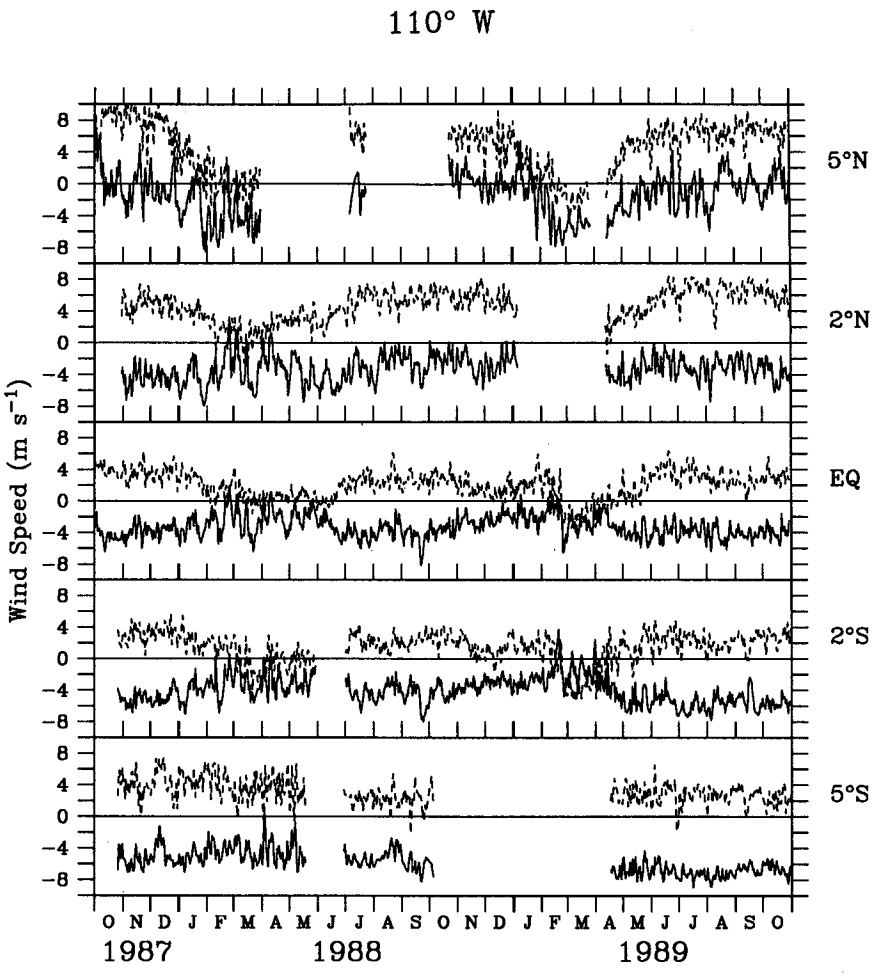

FIG. 2. Same as Fig. 1 but for measurements along 110°W.

At all other sites, the measurements were made with the wind system used on ATLAS (Autonomous Temperature Line Aquisition System) wind and thermistor chain moorings. The ATLAS mooring is described in Hayes et al. (1991). Briefly, wind measurements at 3.8 m above the sea surface are made using a propeller-vane sensor, which is sampled at 2 Hz and vector averaged. The averaging interval varied depending on the electronics used at each location. All ATLAS time series presented here are based on 24-h vector-averaged data, except at 7°N, 140°W where the basic time series is a 2-h vector average. Freitag et al. (1989) compared buoy wind measurements using the VAWR and ATLAS techniques and found no significant differences in the wind statistics.

The time series used in this analysis were collected in 1987–89. This time period encompassed the end of an ENSO warm event (1986–87) and an ensuing cold event (1988). This interannual variability may influence the statistics discussed here; but without significantly longer records, it is not possible to quantify this influence.

In the analyses, data segments without gaps were used in subsampling studies. For estimations of spectra and coherence, approximately 1-yr-long data segments were selected at each site. At some locations, these computations required using records with data gaps; in these cases, the gaps were filled by linear interpolation. The record lengths used in these calculations are indicated in Table 1.

The time series provide a general indication of the surface wind regimes in which the measurements occurred. From the annual mean values in Table 1, it is clear that near the equator the southeast trade winds peak in the region from 140° to 170°W. Equatorial mean zonal wind for the periods chosen was approximately the same (3.0 m s^{-1}) at 110°W and 165°E and nearly doubled at 140° and 170°W. Maximum meridional wind occurred north of the equator at 110°W in the region of the sea surface temperature equatorial front. The wind variability was generally largest in the intertropical convergence zone (ITCZ) north of the equator and in the western Pacific. For example, at 9°N, 140°W, the standard deviation of the

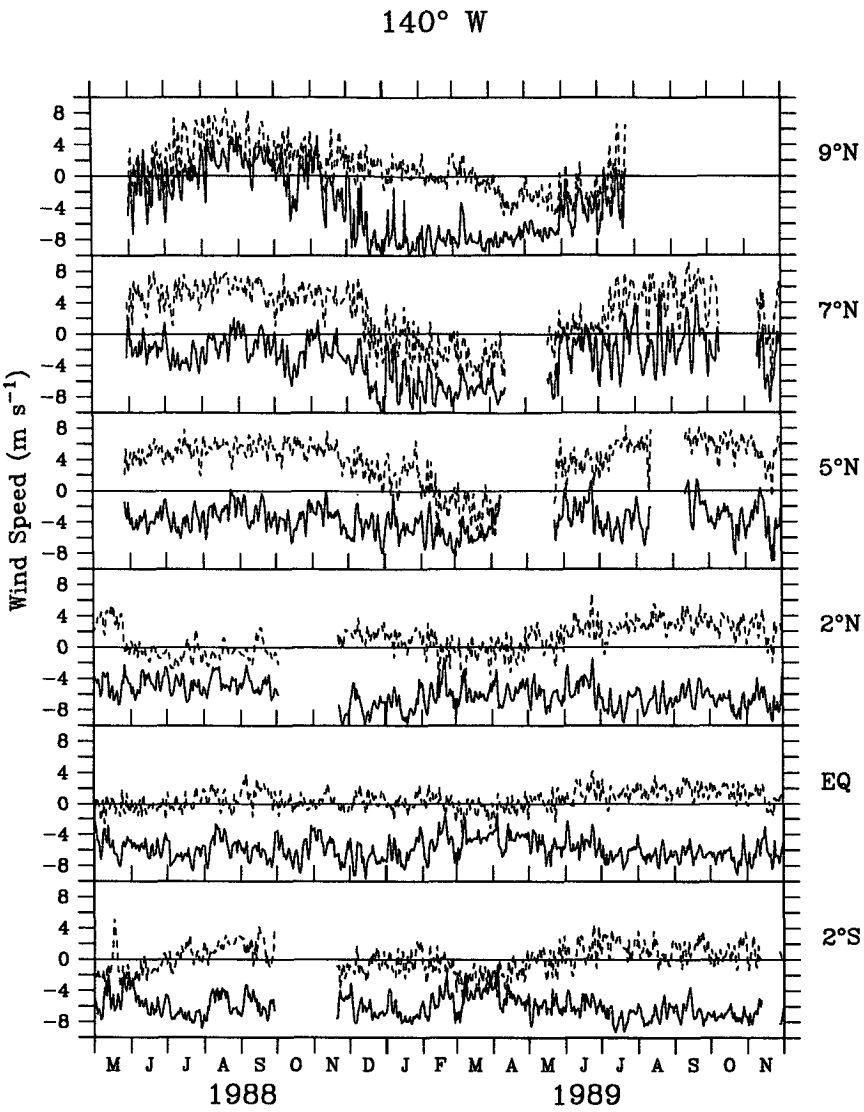

FIG. 3. Same as Fig. 1 but for measurements along 140°W.

zonal wind (4.5 m s^{-1}) exceeded the magnitude of the annual mean by 1.4 m s^{-1}. The high variability in these warm SST regions with large convective activity is not surprising.

In the eastern Pacific, there is an annual cycle in both wind components (Figs. 1 and 2). Climatologically, minimum wind speed occurs in March and maximum in October (Goldenberg and O'Brien 1981). The general features of this climatological cycle were verified in the Halpern (1988b) analysis of buoy measured winds and are apparent in Figs. 1 and 2. In 1989, the meridional wind on the equator at 110° and 125°W reversed sign (becoming northerly) during March, and zonal easterly winds were relatively weak. Periods of westerly wind occurred briefly at both 110° and 125°W in February 1989. In boreal summer and fall, the southeast trades were strong; maximum monthly mean speed on the equator at 110°W was 6 m s^{-1} in September 1988. Year-to-year differences in the annual cycle can be seen by comparing May 1988 and 1989 on the equator at 110°W (Fig. 1). In May 1988, the southeast trade winds were quite weak, while 1 year later the easterly component was well established.

At 170°W (Fig. 1), an annual cycle is still apparent, and the minimal easterly winds appear to occur a month or two later than 110°W. There is, however, a gap in the record in 1989, which makes the annual cycle difficult to resolve. At 165°E (Fig. 4), the climatological annual cycle has northerly winds in boreal winter and maximum southeasterlies in the summer. Our records tend to show this cycle, but the daily time series emphasizes the important contribution of the

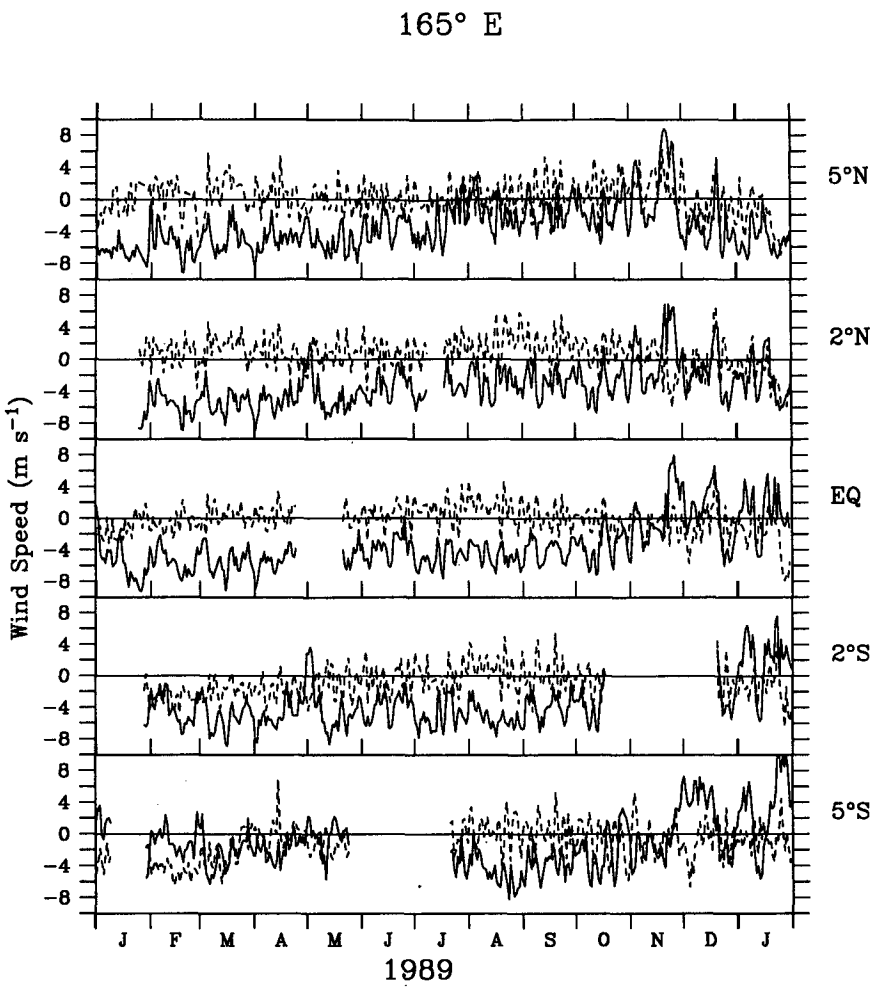

FIG. 4. Same as Fig. 1 but for measurements along 165°E.

high-frequency events. Much of the weakening of zonal wind in November–January was associated with westerly wind bursts.

There is a strong annual cycle in both wind components in the ITCZ from 5° to 9°N in the central Pacific (Fig. 3). Meridional winds become northerly early in the year. The change in direction in 1989 appeared to occur earliest at 7°N and later at 9°N and 5°N. Zonal winds were generally easterly, although there were weak westerly winds in August 1988 at 9°N and August 1989 at 7°N. Again, westerly wind events appear to be important in this annual cycle.

Spectra of the equatorial records at 110°W, 140°W, and 165°E and of the measurements at 7°N, 140°W (Fig. 5) are representative of the variability in the wind regimes covered by the array. These spectra were computed from 1-yr-long records (see Table 1 for dates); prior to spectral calculation, the time series were detrended by joining the end points. The spectral estimates were smoothed using a Daniel window with varying width in frequency space. The 95% confidence intervals for the variance-density spectra are indicated.

The zonal-wind spectra tend to have a broad region of increased variance in the period band from about 5 to 50 days. The increased energy in this band at 165°E compared to the equatorial data in the eastern Pacific is obvious; there is a factor of 6 more energy in the western Pacific. The off-equatorial record at 7°N, 140°W in the ITCZ also had enhanced weekly-to-monthly zonal-wind variance. In the 5–50-day band, the variance was three times larger at 7°N than at 0°, 140°W.

The meridional-wind variance tended to be peaked at higher frequencies. On the equator at 110°W and 140°W, there was increased variance at the diurnal period and in the band from about 2–10 days. At 165°E, a peak at the diurnal period was not apparent, and the band of enhanced variance was broader, extending to about 30 days. At 7°N, 140°W, the enhanced variance was largely between 2 and 10 days.

TABLE 1. Approximately annual mean and standard deviation about the mean of wind components at the nominal locations indicated in the tropical Pacific. The time period of each record is indicated. An asterisk (*) indicates that a gap in the data was filled by linear interpolation. The length of the gap in days is indicated by the number in parentheses. Daily averaged data were used in these computations.

		Mean ($m\ s^{-1}$)		Standard deviation ($m\ s^{-1}$)	
Location	Time	u	v	u	v
5°N, 110°W	29 Oct 1988–28 Oct 1989* (17)	−1.5	4.1	2.7	3.3
2°N, 110°W	30 Oct 1987–30 Oct 1988	−3.5	4.0	1.9	2.0
0°, 110°W	29 Oct 1988–28 Oct 1989	−3.2	1.8	1.4	1.9
2°S, 110°W	29 Oct 1988–28 Oct 1989	−4.1	1.2	1.9	2.2
5°S, 110°W	26 Oct 1987–4 Oct 1988* (41)	−5.0	3.3	1.3	1.7
0°, 125°W	29 Oct 1988–28 Oct 1989	−4.6	1.3	1.3	1.7
9°N, 140°W	31 May 1988–8 Apr 1989	−3.1	2.0	4.5	2.5
7°N, 140°W	31 May 1988–12 Apr 1989	−3.7	2.6	2.9	3.8
5°N, 140°W	29 May 1988–7 Apr 1989	−4.0	3.2	1.7	3.1
2°N, 140°W	1 Dec 1988–30 Nov 1989	−6.4	1.6	1.5	1.9
0°, 140°W	29 Oct 1988–28 Oct 1989	−5.8	0.7	1.5	1.3
2°S, 140°W	19 Nov 1988–11 Nov 1989	−6.2	0.0	1.4	1.8
0°, 170°W	15 May 1988–2 May 1989	−6.4	0.0	1.4	1.1
5°N, 165°E	30 Jan 1989–29 Jan 1990	−3.3	0.2	3.0	2.2
2°N, 165°E	30 Jan 1989–29 Jan 1990* (9)	−3.3	0.7	2.7	2.1
0°, 165°E	30 Jan 1989–29 Jan 1990* (26)	−3.0	−0.1	3.2	1.9
2°S, 165°E	30 Jan 1989–29 Jan 1990* (63)	−2.8	−0.3	3.4	2.3
5°S, 165°E	30 Jan 1989–29 Jan 1990* (57)	−1.3	−0.9	3.2	2.2

Again, the variance in this band was larger on the equator in the western Pacific and in the ITCZ.

The fraction of the meridional-wind variance at periods shorter than 1 day was larger in the western Pacific (about 22% at 0°, 165°E), compared to the eastern or central Pacific (10% to 15% at 110° and 140°W). This relatively large high-frequency contribution in the western Pacific indicates that subsampling studies

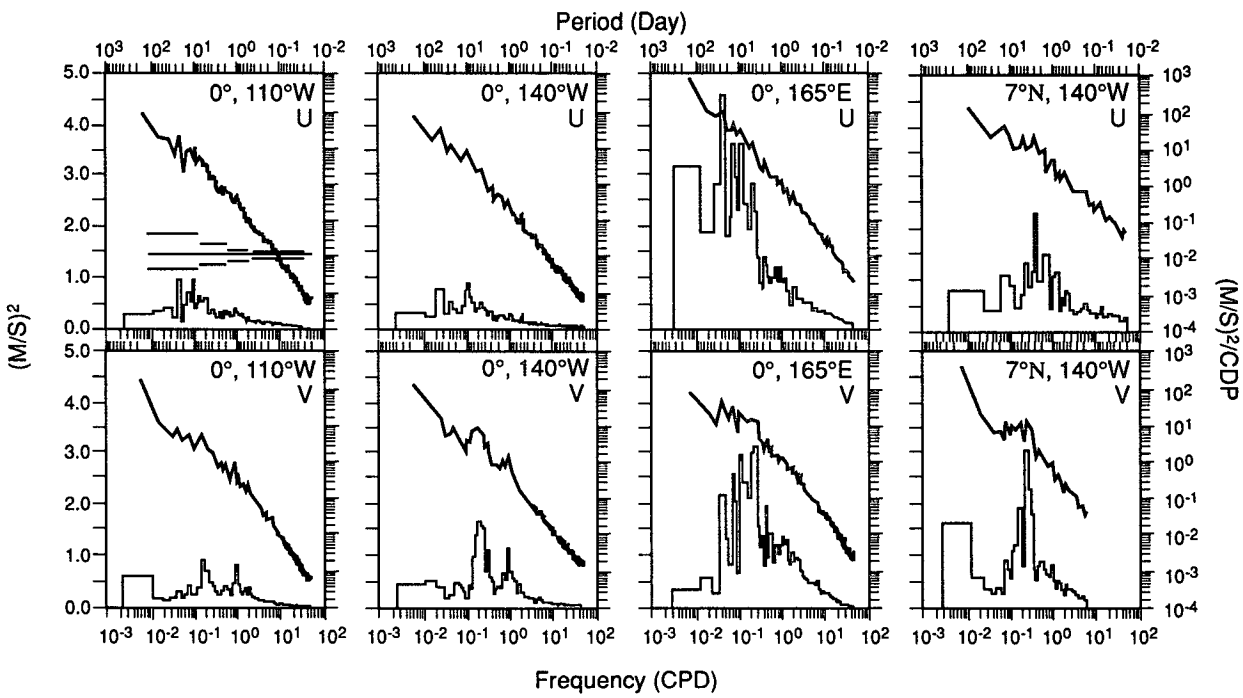

FIG. 5. Spectra of zonal- (u) and meridional- (v) wind variance at three locations along the equator (110°W, 140°W, and 165°E) and at 7°N, 140°W. Both variance-preserving (histogram and scale on left) and variance-density (scale on right) spectra are shown. Error bars shown for 0°, 110°W apply to all variance-density spectra.

should be limited to the high-resolution time series. These time series will also be used to estimate the influence of daily averaging on derived variables such as wind stress.

3. Wind coherence

Zonal and meridional scales of wind coherence were examined using approximately 1-yr-long records of daily averaged winds. In all cases, the time series was prewhitened by joining the end points before Fourier transforms were computed. Coherence estimates were based on band-averaging individual frequency estimates. Coherence, not coherence squared, is used to indicate the correlated variability. Simultaneous measurements were not made at all sites (Figs. 1–4); thus, the time periods available for comparison varied among the sites. For this reason, comparison of coherence scales at different locations (e.g., along 110°W and 165°E) may be influenced by temporal nonstationarity as well as the geographical variability of the wind field.

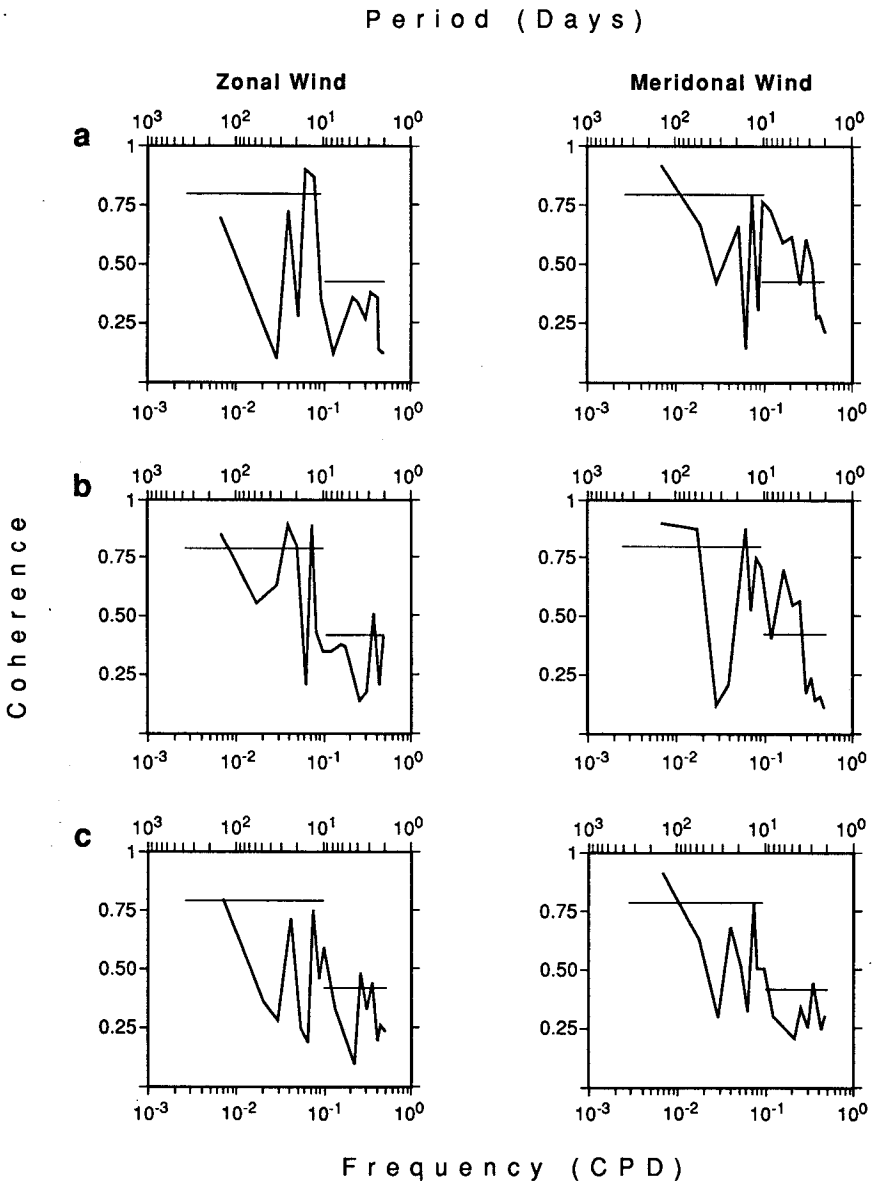

FIG. 6. Zonal coherence of wind components separated by 15° and 30° longitudinally in the eastern to central equatorial Pacific. Horizontal lines on coherence plots indicate 95% confidence level for nonzero coherence; (a) 110°W compared with 125°W; (b) 125°W compared with 140°W; (c) 110°W compared with 140°W.

TABLE 2. Zonal coherence of surface wind components along the equator and along 7°N. Coherence estimates are for bands where each wind component had significant energy. Zonal-wind coherences are for the period band 5–50 days (95% significance level approximately 0.22) and meridional coherences are for the period band 2–10 days (95% significance level approximately 0.15).

	Zonal wind	Meridional wind
	Along the equator	
110°W–125°W	0.20	0.37
125°W–140°W	0.44	0.38
110°W–140°W	0.03	0.15
140°W–170°W	0.24	0.18
170°W–165°E	0.14	0.13
	Along 7°N	
132.5°W–140°W	0.45	0.28
140°W–147.5°W	0.72	0.44
132.5°W–147.5°W	0.32	0.15

a. Zonal coherence scales

Along the equator, the time series in Fig. 1 were compared. For example, Fig. 6 shows the coherence between equatorial records at 110°, 125°, and 140°W. The 95% significance level for nonzero coherence is indicated by the horizontal lines on the figures. For periods longer (shorter) than 10 days, 4 (16) frequency estimates were averaged to obtain the coherence estimates.

The results in Fig. 6 generally agree with Halpern (1988b). For separations of 15° of longitude, zonal winds were only significantly coherent at a few isolated frequencies. Meridional winds were, however, coherent in the 3–10-day period band, which contains most of the meridional-wind energy (Fig. 5). For 30° longitudinal separations, coherence was low for both wind components.

The zonal coherence estimates are summarized in Table 2, which displays the band-averaged coherence of zonal winds in the 5–50-day period band (average of at least 63 frequency estimates, 95% significance level 0.22) and meridional winds in the 2–10-day period band (average of at least 133 frequency estimates, 95% significance level 0.15). These bands were chosen to represent the energetic portion of the spectra for each component (Fig. 5). Along the equator, the coherence was larger in the case of the trade-wind regime from 125° to 170°W than to the east or west. Even at the 15° longitude separation, however, the coherence was not large, and coherence squared indicated that only about 15%–20% of the total variance could be linearly related.

Off the equator, zonal coherence was examined using three buoys deployed along 7°N as part of a study of the North Equatorial Counter Current. Along this latitude, measurements were available at 132.5°, 140°, and 147.5°W. Coherence was again summarized by the band averages in Table 2. For the overlapping records available, coherence was larger between 140° and 147.5°W than between 140° and 132.5°W; however, all band-averaged coherence over 7.5° longitude was significant and zonal-wind was also significantly coherent over the 15° separation. There was not a clear difference in zonal-wind coherence over 15° longitude separation on the equator compared to 7°N; however, meridional wind appears to be more coherent along the equator than along 7°N.

b. Meridional coherence scales

Meridional coherence scales were examined using the moored arrays along 110°W, 140°W, and 165°E. In the eastern Pacific (Fig. 7), zonal wind was fairly coherent within 2° of the equator over a broad band from about 2 to 20 days. The bandwidth of this coherent structure decreased with larger separations, but variability with periods near 10 days were coherent over 5° latitude. Meridional winds within 2° of the equator were also significantly coherent for a variety of periods less than 10 days. At 5° separation, a coherence peak near a 5-day period remained significant.

At 165°E in the western Pacific, zonal winds were mostly coherent (Fig. 8) over 2° latitude separation in the band of periods from about 5 to 40 days. At 5° latitude separation, zonal-wind coherence was confined to a few peaks (near 3-, 7-, and 20-day periods south of the equator and from 4 to 10 days north of the equator). Meridional winds were generally coherent in the period band from 3 to 8 days. The coherence peak near 4–5 days remained well above the 95% significance level even for 5° separation. This peak may be related to the equatorial mixed Rossby–gravity-wave energy previously detected in this period range in the western Pacific (Wallace 1971). The phase difference of the coherent signal was small (less than 45°) for all latitudes compared.

The structure of the meridional coherence of surface winds is summarized in Table 3, where the band-average coherences for zonal and meridional winds are shown. For separations of 2° latitude near the equator, zonal-wind coherence was about 0.7 (95% significance level 0.22) and meridional-wind coherence varied from 0.56 to 0.75 (95% significance level 0.15). Meridional-wind coherence across the equator was smallest in the eastern Pacific (110°W).

Table 3 also shows the coherence estimates in the region of the ITCZ along 140°W. Both zonal and meridional winds were significantly coherent between 5° and 9°N, but the square of this coherence indicates that only about 10% of the variance in the two signals was linearly related. For 2° separations in the ITCZ, 30%–50% of the variance in the zonal- and meridional-wind bands were related. The meridional-wind scale in this region appears to be somewhat smaller than

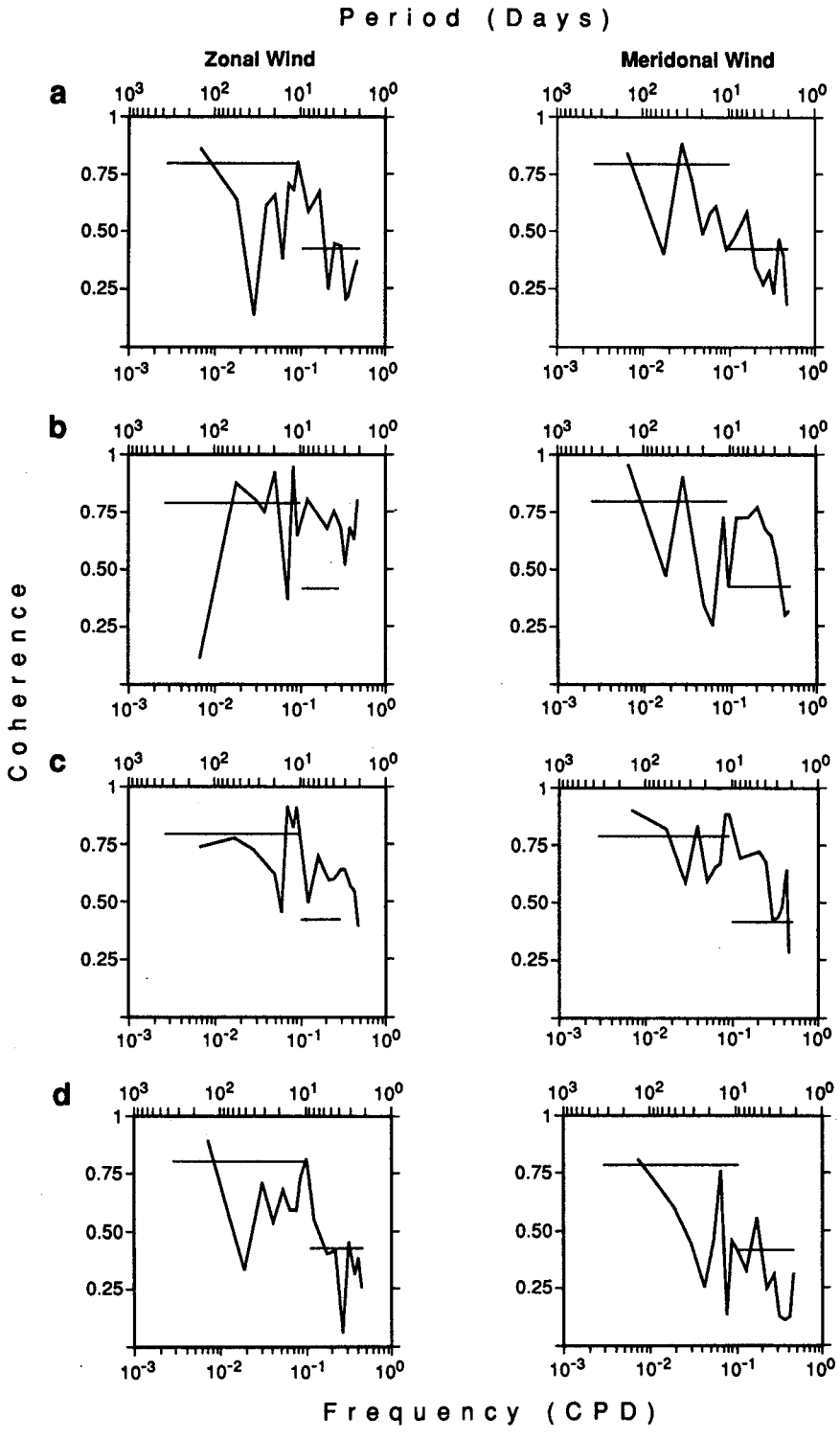

FIG. 7. Meridional coherence of wind components along 110°W. Horizontal line on coherence plots indicates 95% confidence level for nonzero coherence. Equatorial records are compared with (a) 5°N, (b) 2°N, (c) 2°S, and (d) 5°S.

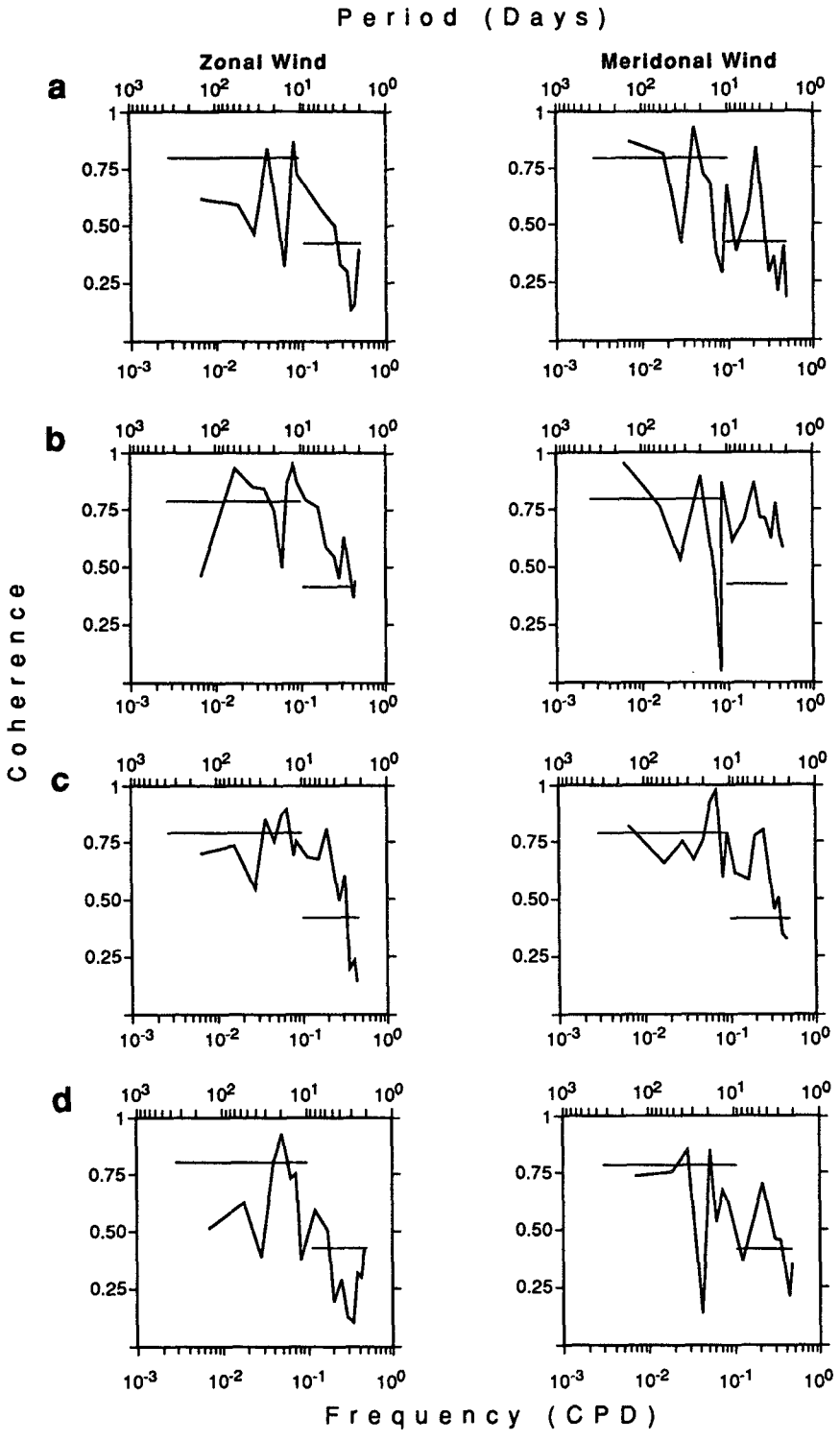

FIG. 8. Same as Fig. 7 but for measurements along 165°E.

TABLE 3. Meridional coherence of surface wind components along four longitudes. Coherence estimates are for bands where each wind component had significant energy. Zonal-wind coherences are for the period band 5–50 days (95% significance level approximately 0.2) and meridional-wind coherences are for the period band 2–10 days (95% significance level approximately 0.15).

	Zonal wind	Meridional wind
	Along 110°W	
0°–2°N	0.79	0.61
0°–2°S	0.62	0.56
0°–5°N	0.30	0.38
0°–5°S	0.50	0.20
	Along 140°W	
0°–2°N	0.71	0.70
0°–2°S	0.75	0.76
0°–5°N	0.53	0.38
5°N–9°N	0.30	0.30
7°N–9°N	0.54	0.54
5°N–7°N	0.71	0.55
	Along 165°E	
0°–2°N	0.72	0.75
0°–2°S	0.69	0.75
0°–5°N	0.41	0.56
0°–5°S	0.48	0.48

near the equator; however, the difference between the two regions is not large.

4. Temporal sampling

a. Monthly mean data

Because of the sparseness of data coverage in the tropical Pacific, most analyses of shipboard wind data (Goldenberg and O'Brien 1981; Harrison 1989) rely on monthly averaged winds. As noted above, Halpern (1988a) used buoy winds at three sites along the equator to estimate the effects of aliasing on monthly mean wind speed. He found that at all locations, approximately ten random measurements each month, were required in order to achieve monthly mean wind estimates accurate to within 1.0 m s^{-1}. Legler (1991) extended the investigation of temporal sampling to consider 5-day mean values and to include midlatitude measurements. He developed second-order polynomials, which estimated the number of observations needed to obtain a given wind-speed accuracy (either 0.5 or 1.0 m s^{-1}) in terms of the standard deviation of the hourly data about the 5- or 30-day means.

The new high-resolution time series on the equator at 110°W, 140°W, and 165°E and at 7°N, 140°W were used to reexamine the question of temporal sampling. These calculations represent new oceanographic regimes (the western Pacific and ITCZ) and different time periods from those considered in previous studies. Following Halpern (1988a) and Legler (1991), Monte Carlo simulations were used to estimate the monthly mean wind speed and wind stress from subsampled time series. These simulations were compared to the "true" monthly mean obtained from the full time series. Results agreed well with the previous studies for the eastern and central Pacific; an accuracy of 1 m s^{-1} in monthly mean wind speed required about ten samples per month at 0°, 110°W and 0°, 140°W. In the western Pacific and near the ITCZ, the wind variability is larger, and 25–30 samples per month were required to reduce the monthly mean wind speed uncertainty to less than 1 m s^{-1}. This increase in the number of samples is consistent with the relations between sampling and the standard deviation of the time series developed by Halpern (1988a) or Legler (1991).

b. Daily mean data

Hayes et al. (1991) discuss plans to deploy an extensive array of ATLAS wind and thermistor chain moorings in the tropical Pacific Ocean as part of the Tropical Ocean Global Atmosphere (TOGA) Program. The standard ATLAS mooring in the new array telemeters, in real-time, daily vector-averaged values of wind components, computed from 24 hourly samples. Each hourly sample is itself a vector average over 6 min of the 2-Hz basic sampling of wind speed and direction. These hourly values are also telemetered in real time; however, because of the frequency of satellite passes and the duty cycle of the transmitter, only a few of the hourly data are received (the remainder are available from the internal recording system on the mooring after the system is recovered). Thus, the primary wind dataset for driving ocean models in near real time will be the daily averaged wind components. Daily values of wind stress and wind speed estimated from daily averaged wind components may differ slightly from daily values estimated from hourly data, which are subsequently averaged. This difference is examined here.

The equatorial measurements at 110°W, 140°W, and 165°E were used to compute vector-averaged wind components from high-resolution (one 15-min-average sample each hour) and low-resolution (daily averaged) time series. Wind speed and wind stress were then computed from these two time series, and the high-resolution estimates were averaged to form a daily estimate that could be compared to the low-resolution estimate. At 110°W wind speed, both pseudostress components calculated by the two methods were highly correlated ($r^2 > .99$) and rms differences were quite small (0.24 m s^{-1} for speed and about 1 m^2 s^{-2} for pseudostress components). The comparison at 0°, 140°W was similar to the 110°W result. Even at 165°E, where there is more variance at periods less than 1 day,

the correlations were good ($r^2 \geq .95$), and the rms difference in wind speed was only 0.72 m s^{-1}. The maximum rms error in pseudostress was 4.2 m^2 s^{-2} (corresponding to a wind-stress estimate of 0.007 N m^{-2}). These errors are small compared to other uncertainties in wind stress; for example, Halpern (1988b) notes that near the equator, the surface current can introduce 20% errors in wind-stress computation. It thus appears that little information is lost if daily averaged, rather than hourly wind components, are used to estimate daily wind speed and stress.

5. Summary

Analysis of moored buoy measurements in the tropical Pacific corroborates and extends earlier estimates of the spatial and temporal scales required to adequately sample the surface wind field. Based on coherence estimates in the eastern, central, and western Pacific, a minimally coherent array would require measurements with separations of 10°–15° longitude and 2°–3° latitude. Such an array would define the large-scale structure of the wind field; however, even this resolution would limit the ability to study processes associated with mesoscale events, for example, the westerly wind bursts in the western Pacific.

Temporal sampling requirements depend on the processes being studied. If monthly mean wind is adequate, then at least ten surface wind measurements per month are required throughout the tropical Pacific. In the western Pacific, this minimal criteria increases, and almost daily sampling is needed. The study showed that daily wind speed and stress can be calculated from daily mean wind components with little loss of accuracy.

The analysis was limited by the time periods available for comparison. Since the surface wind field of the tropical Pacific has considerable interannual variability, which may influence the higher-frequency variance (Luther and Harrison 1984), results of studies such as this are dependent on the periods measured. Long time series from the TAO (tropical atmosphere ocean) array (Hayes et al. 1991) will allow a more definitive study of the space–time variability of the surface wind field.

Acknowledgments. We are grateful to Dr. Michael J. McPhaden, who shared the wind measurements on the current-meter moorings with us. We appreciate the technical assistance of Doug Fenton, John LoConte, Rick Miller, Ben Moore, Julia Neander, and Andy Shepherd for instrument preparation and operations at sea. Nancy Soreide was very helpful in data processing. Paul Freitag processed the current-meter mooring data. This work has been supported in part by NOAA's Equatorial Pacific Ocean Climate Study (EPOCS) and the U.S. TOGA Project Office. This is Pacific Marine Environmental Laboratory contribution 1284.

REFERENCES

Freitag, H. P., M. J. McPhaden, and A. J. Shepherd, 1989: Comparison of equatorial winds as measured by cup and propeller anemometers. *J. Atmos. Oceanic Technol.*, **6**, 327–332.

Goldenberg, S. B., and J. J. O'Brien, 1981: Time and space variability of tropical Pacific wind stress. *Mon. Wea. Rev.*, **109**, 1109–1207.

Halpern, D., 1988a: On the accuracy of monthly mean wind speeds over the equatorial Pacific. *J. Atmos. Oceanic Technol.*, **5**, 362–367.

——, 1988b: Moored surface wind observations at four sites along the Pacific equator between 140° and 95°W. *J. Climate*, **1**, 1251–1260.

Harrison, D. E., 1989: On climatological monthly mean wind stress and wind stress curl fields over the World Ocean. *J. Climate*, **2**, 57–70.

——, 1992: The tropical Pacific seasonal cycle of SST: An ocean circulation model simulation and its thermal balances. *J. Climate*, submitted.

——, and D. Luther, 1990: Surface winds from tropical Pacific islands: Climatological statistics. *J. Climate*, **3**, 251–271.

——, W. S. Kessler, and B. S. Giese, 1989: Ocean circulation model hindcasts of the 1982–83 El Niño: Thermal variability along the ship-of-opportunity tracks. *J. Phys. Oceanogr.*, **19**, 397–481.

——, B. S. Giese, and E. S. Sarachik, 1990: Mechanisms of SST change in the equatorial waveguide during the 1982–83 ENSO. *J. Climate*, **3**, 173–188.

Hayes, S. P., L. J. Mangum, J. Picaut, A. Sumi, and K. Takeuchi, 1991: TOGA-TAO: A moored array for real-time measurements in the tropical Pacific Ocean. *Bull. Amer. Meteor. Soc.*, **72**, 339–347.

Hellerman, S., and M. Rosenstein, 1983: Normal monthly wind stress over the World Ocean with error estimates. *J. Phys. Oceanogr.*, **13**, 1093–1104.

Legler, D. M., 1991: Errors of five-day mean surface wind and temperature conditions due to inadequate sampling. *J. Atmos. Oceanic Technol.*, **8**, 705–712.

Lukas, R., S. P. Hayes, and K. Wyrtki, 1985: Equatorial sea level response during the 1982–83 El Niño. *J. Geophys. Res.*, **89**, 10 425–10 430.

Luther, D. S., and D. E. Harrison, 1984: Observing long-period fluctuations of surface winds in the tropical Pacific: Initial results from island data. *Mon. Wea. Rev.*, **112**, 285–302.

McPhaden, M. J., H. P. Freitag, S. P. Hayes, B. A. Taft, Z. Chen, and K. Wyrtki, 1988: The response of the equatorial Pacific Ocean to a westerly wind burst in May 1986. *J. Geophys. Res.*, **93**(C9), 10 589–10 603.

Reynolds, R. W., K. Arpe, C. Gordon, S. P. Hayes, A. Leetmaa, and M. J. McPhaden, 1989: A comparison of tropical Pacific surface wind analyses. *J. Climate*, **2**, 105–111.

Wallace, J. M., 1971: Spectral studies of tropospheric wave disturbances in the western tropical Pacific. *Rev. Geophys. Space Phys.*, **9**, 557–619.